

ESI: On the acoustically induced fluid flow in particle separation systems employing standing surface acoustic waves - Part II

Sebastian Sachs, Christian Cierpka, and Jörg König
*Institute of Thermodynamics and Fluid Mechanics,
Technische Universität Ilmenau, P.O. Box 100565, D-98684 Ilmenau, Germany*

Movie M1: Experimental results of the acoustically induced fluid flow at the beginning of the sSAW (ROI 1) for a channel height of $185\ \mu\text{m}$, a SAW wavelength of $20\ \mu\text{m}$ and an electrical power of $154\ \text{mW}$ visualized by streamlines in the temporally and spatially averaged velocity fields in a 3D view. The beginning of the IDT is indicated by a red dashed line.

Movie M2: Streamlines in the temporally and spatially averaged velocity fields at the end of the sSAW at a channel height of $185\ \mu\text{m}$, a SAW wavelength of $20\ \mu\text{m}$, and an electrical power of $154\ \text{mW}$. The end of the IDT is highlighted by a red dashed line.

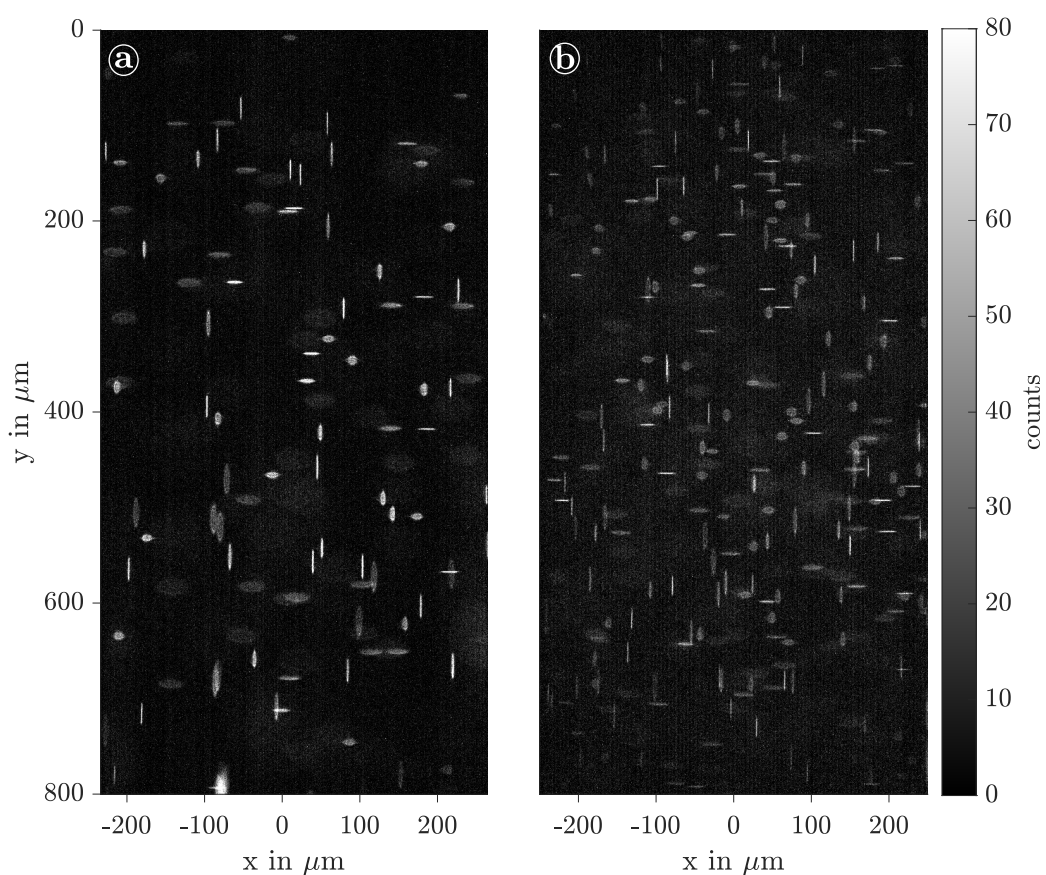


FIG. S1. Experimentally acquired images using astigmatism particle tracking velocimetry (APTV) at the beginning (ROI 1) of the pseudo-standing surface acoustic wave (sSAW) for a wavelength of $150\ \mu\text{m}$ and a channel height of $185\ \mu\text{m}$. Spherical polystyrene particles with radii of $0.57\ \mu\text{m}$ (a) and $0.225\ \mu\text{m}$ (b) were used with a seeding density below $5.1 \times 10^{-6}\ \%$ v/v and $1.0 \times 10^{-6}\ \%$ v/v, respectively. Overall, the seeding density remained low to allow for the detection of particle positions and shapes as well as to reduce particle-particle interactions. When reducing the particle radius to $0.225\ \mu\text{m}$, the signal-to-noise ratio further decreased.

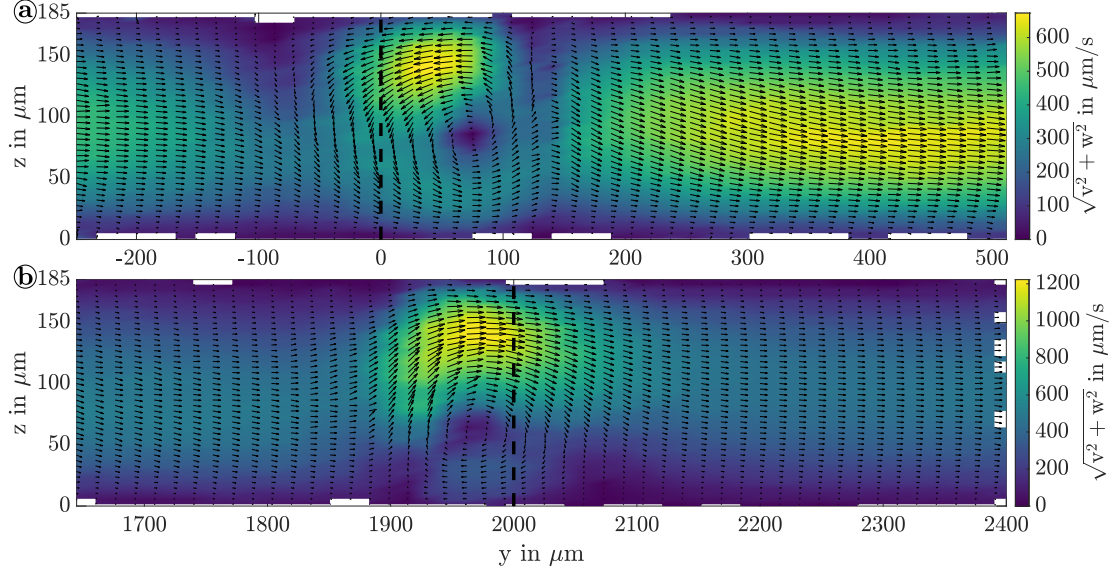


FIG. S2. Experimentally determined fluid flow in sectional planes at the beginning (a, $x_0 = 0 \mu\text{m}$) and end (b, $x_0 = 130 \mu\text{m}$) of the standing surface acoustic wave (sSAW) with a wavelength of $20 \mu\text{m}$, a channel height of $185 \mu\text{m}$, and an electric power of 154 mW . The color scale denotes the absolute in-plane velocity in the plane shown. The dashed lines indicate the beginning and the end of the IDTs.

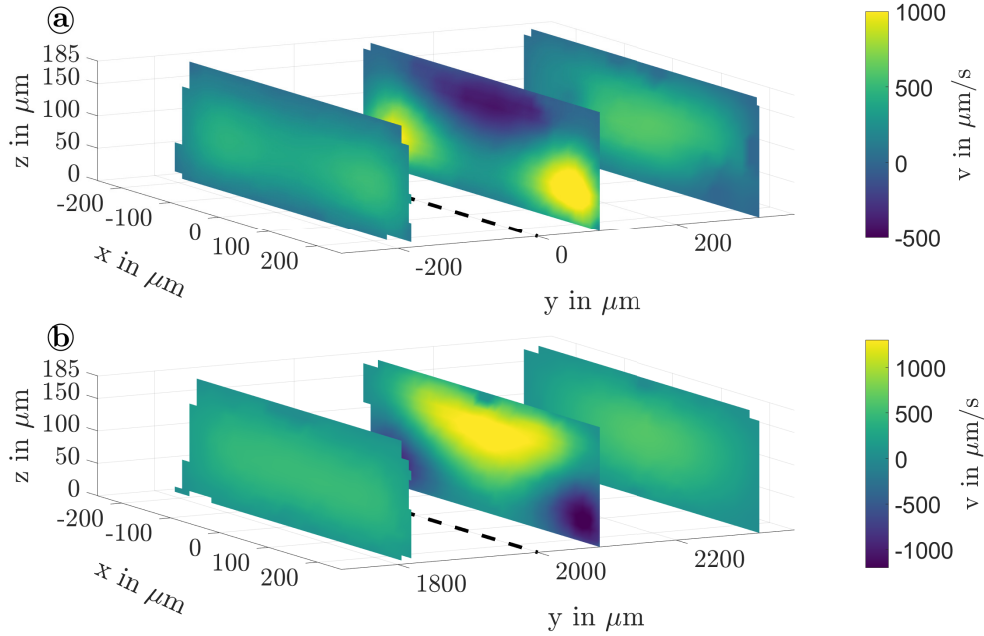


FIG. S3. Velocity component $v(x, y_i, z)$ in main flow direction in sectional planes around the beginning (a) and the end of the sSAW (b) for a wavelength of $20 \mu\text{m}$, a channel height of $185 \mu\text{m}$ and an electrical power of 154 mW . Recirculations and separated velocity maxima occur only near the edges of the IDT at $y = 0 \mu\text{m}$ and $y = 2000 \mu\text{m}$ (highlighted by dashed lines).

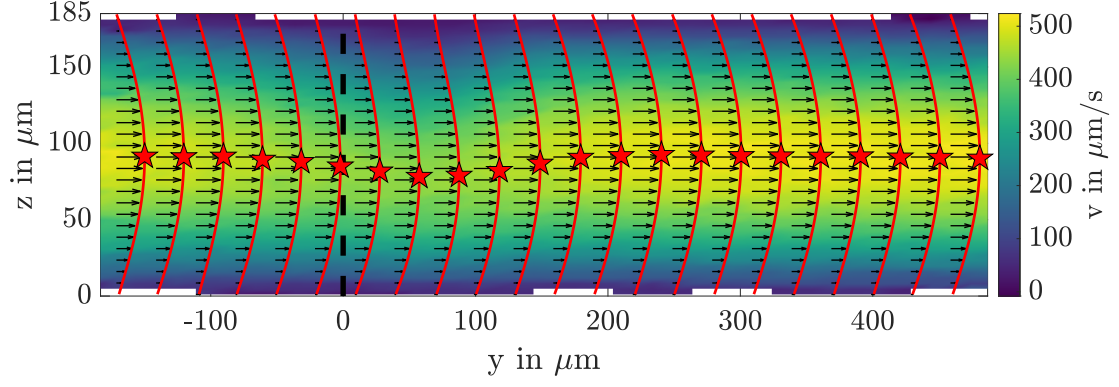


FIG. S4. Vector field $(0, v, 0)'$ with velocity component $v(x_0, y, z)$ in main flow direction along the channel center ($x_0 = 0 \mu\text{m}$) for a SAW wavelength of $20 \mu\text{m}$, a channel height of $185 \mu\text{m}$ and an electrical power of 29.85 mW . The velocity profiles $v(x_0, y_i, z)$ at the location (x_0, y_i) are approximated by fourth order polynomials (red curves). The positions of maximum velocity are denoted by red stars.